Charge-Density Study of Methane Di(triimido)sulfonic Acid $H_2C\{S(NtBu)_2(NHtBu)\}_2$—the NR Analogue of $H_2C\{S(O)_2(OH)\}_2$**

Dirk Leusser, Bernhard Walfort, and Dietmar Stalke*

Methane disulfonic acid $H_2C\{S(O)_2(OH)\}_2$ was synthesized for the first time more than 160 years ago.[1] Since then, this very strong acid[2] has been structurally studied because the hydrates form stable dihydroxonium salts $[(H_3O)_2\{(O_3S)_2CH_2\}]_\infty$ with strong hydrogen bonds.[3] The methane disulfonate dianion $H_2C(SO_3)_2^{2-}$ shows both unidentate (terminal) and bidentate (O,O chelating) coordination in many metal salts which leads to infinite solid-state structures.[4] Both features of disulfonates were recently employed in crystal engineering; $H_2C(SO_3)_2^{2-}$ ions serve as molecular pillars to separate two-dimensional galleries in tunable, hydrogen-bonded, nanoporous materials.[5] We set out to switch all six oxygen atoms in this basic compound isoelectronically to NR groups to generate molecules that would be soluble in hydrocarbons rather than exist as infinite solid-state salts.[6]

Herein we present dilithium methane di(triimido)sulfonate $[(thf)_2Li_2\{((NtBu)_3S)_2\}_2CH_2]$ (**1**), and methane di(triimido)-sulfonic acid, $H_2C\{S(NtBu)_2(NHtBu)\}_2$ (**2**), the NR analogues of $H_2C(SO_3)_2^{2-}$ and $H_2C\{S(O)_2(OH)\}_2$, respectively. Since **2** displays three different S–N bonding modes at each sulfur(VI) atom (one formal S–N(H)R single bond and two formal S=NR bonds, one of them involved in intramolecular hydrogen bonding), this is the ideal system in which to study the electron density of S–N bonds. We analyzed experimentally the charge-density distribution, $\rho(\boldsymbol{r})$, from high-resolution, low-temperature X-ray data and subsequent multipole refinement.[7]

The direct route corresponding to the established Strecker synthesis[1c] to give alkane disulfonates starting from dibromoalkanes and sodiumsulfite is precluded by the complex redox processes of the required dilithium (triimido)sulfite. However, alkylene (triimido)sulfate $[(donor)Li_2\{(CH_2)S(NtBu)_3\}]$,[8] the carba/imido analogue of the SO_4^{2-} ion, can readily be synthesized by deprotonation of $H_3CS(NtBu)_3$[9] with methyllithium. Addition of one equivalent of $S(NtBu)_3$ to the sulfur(VI)-ylide gives **1**. Subsequent protonation and salt elimination by *tert*-butylammonium chloride yields **2** (Scheme 1).

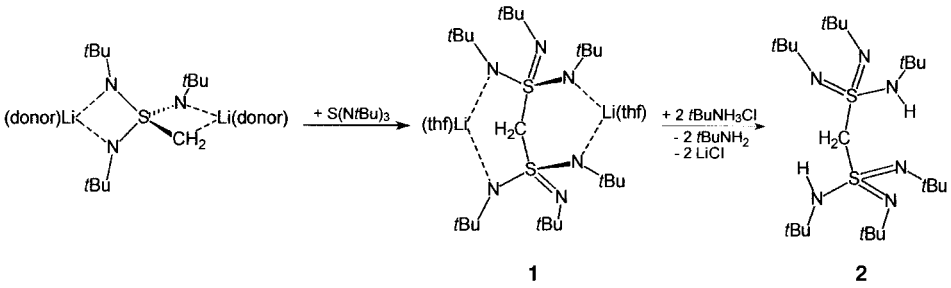

Scheme 1. Synthesis of **1** and **2**.

Unlike the known Ca^{2+}, Cd^{2+}, Ag^+, or K^+ salts of methane disulfonates,[4] **1**, forms donor-base-stabilized molecules (Figure 1, left). Both lithium cations are each coordinated, as if in pincers, by two opposing nitrogen atoms of both

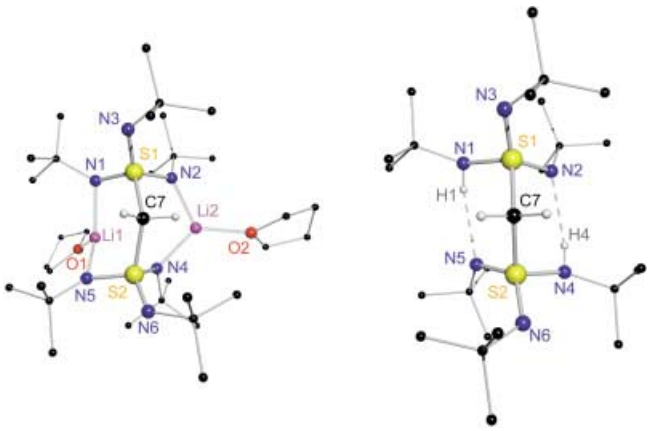

Figure 1. Left: Crystal structure of **1**. Selected bond lengths [Å] and angles [°]: S1-N1 1.572(3), S1-N2 1.568(4), S1-N3 1.527(3), S2-N4 1.519(3), S2-N5 1.558(3), S2-N6 1.579(3), S1-C7 1.847(4), C7-S2 1.845(4); S1-C7-S2 126.7(2); right: crystal structure of **2**. Selected bond lengths [Å] and angles [°] after multipole refinement: S1-N1 1.6494(2), S1-N2 1.5278(2), S1-N3 1.5179(2), S2-N4 1.6494(2), S2-N5 1.5280(3), S2-N6 1.5174(3), S1-C7 1.8161(2), C7-S2 1.8166(2); S1-C7-S2 122.20(10), N1,4-H1,4 1.032, average H1,4 ··· N5,2 2.142(13), average N-H ··· N 142.8(2).

staggered $S(NR)_3$ moieties.[10] Additional complexation of a single THF molecule leaves both metals trigonal pyramidally coordinated. On average the Li1–N1,5 bonds are considerably longer than the Li2–N2,4 bonds (2.033(11) vs. 1.939(11) Å). The longer Li–N bonds result in shorter average S–N(Li) bonds and vice versa (1.564(5) vs. 1.576(5) Å). The nitrogen atoms of the pendant imido ligands (N3,6) afford the shortest S–N bonds as there is no competition for the electron density from the metal centers (S1–N3, S2–N6: av. 1.523(5) Å). The average S1,2–C7 bond length with 1.847(4) Å is 0.08 Å longer than the S–C bond in the methyl (triimido)sulfonates.[9] The unprecedented wide S-C-S angle of 126.7(2)° reflects the considerable steric stain between the

[*] Prof. Dr. D. Stalke, Dipl.-Phys. D. Leusser, Dr. B. Walfort
Institut für Anorganische Chemie
Universität Würzburg
Am Hubland, 97074 Würzburg (Germany)
Fax: (+49) 931-888-4619
E-mail: dstalke@chemie.uni-wuerzburg.de

[**] This work was supported by the Deutsche Forschungsgemeinschaft and the Fonds der Chemischen Industrie. The discussions in the Würzburger Graduiertenkolleg "Elektronendichte" were very stimulating. We thank one of the referees for valuable comments.

Supporting information for this article is available on the WWW under http://www.angewandte.com or from the author.

  1433-7851/02/4112-2079 $ 20.00+.50/0

two triimidosulfonate groups which is reinforced by metal coordination.

In the crystal structure of **2**, both lithium ions in **1** are replaced by hydrogen atoms employed in intramolecular N-H···N hydrogen bonding (Figure 1, right). Three different types of S–N bonds result: two undisturbed formal S=N bonds (S1–N3, S2–N6: av. 1.5177(3) Å); two slightly elongated formal S–N double bonds involved in hydrogen bonding (S1–N2, S2–N5: av. 1.5279(3) Å) and two formal S–N(H) single bonds (S1–N1, S2–N4: av. 1.6494(2) Å). Following the Lewis notation the molecule has to be written in accord with the mesomeric structure **a** (Scheme 2) with two S=N bonds at each sulfur center to avoid formal charges in **b** (Pauling's verdict). However, that would imply valence expansion and d-orbital participation at the sulfur atom. We experimentally demonstrated that the form **b** is more appropriate to describe the bonding in the molecule.

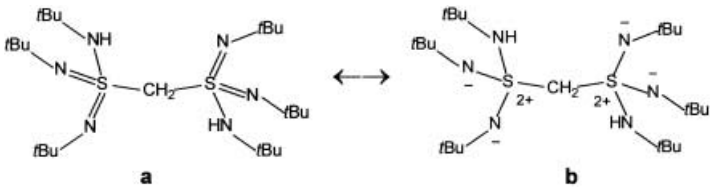

Scheme 2. The two resonance structures of **2**.

To elucidate the charge-density distribution in **2**, especially the bonding situation of the three distinct S–N bonds, we performed a multipole refinement, with the formalism from Hansen and Coppens,[11, 12] based on 100 K high-resolution data up to $(\sin\Theta/\lambda)_{max} = 1.11$ Å^{-1} ($2\Theta_{max} = 104^\circ$ for $Mo_{K\alpha}$, $d =$ 0.45 Å). The resulting topological analysis of the charge-density distribution $\rho(\boldsymbol{r})$ is presented.[13] To characterize the S–N bonds we have analyzed $\rho(\boldsymbol{r})$ and the Laplacian $\nabla^2\rho(\boldsymbol{r})$ in terms of Bader's theory of "atoms in molecules".[14] We found all anticipated $(3,-1)$ *b*ond *c*ritical *p*oints (BCPs) in the bonding regions of the molecule, including two intramolecular $(3,-1)$ BCPs between the N(H) hydrogen and the opposing formally double-bonded nitrogen atoms. All the S–N BCPs are located closer to the less-electronegative sulfur atom (see Table 1). Two $(3,+1)$ ring critical points are located in the six-membered ring made up from the two sulfur and nitrogen atoms, the bridging CH_2 carbon atom, and the N(H) hydrogen atom. A comparison of the densities $\rho(\boldsymbol{r}_{BCP})$, the algebraic sum of the eigenvalues (λ_i) of the Hessian matrix, $\nabla^2\rho(\boldsymbol{r}_{BCP})$ and the ellipticities ε_{BCP} ($\varepsilon_{BCP} = \lambda_1/\lambda_2 - 1$) at the BCPs of the S–N and S–C bonds is presented in Table 1.

Table 1. Topology of the S–N and S–C bonds in **2**.[a]

	d (A-B)	*d* (A-BCP)	*d*(BCP-B)	$\rho(\boldsymbol{r}_{BCP})$	$\nabla^2\rho(\boldsymbol{r}_{BCP})$	ε_{BCP}
S1-N1	1.650	0.780	0.870	1.89(2)	−13.41(7)	0.11
S1=N2	1.530	0.718	0.812	2.31(3)	−16.60(9)	0.10
S1=N3	1.520	0.718	0.802	2.37(3)	−16.44(9)	0.06
S1-C7	1.817	0.984	0.833	1.45(2)	−8.01(4)	0.09

[a] *d*(A-B): distance between atoms A and B along the bondpath in Å; *d*(A-BCP), *d*(BCP-B): distance between BCP and atom A and B, respectively; $\rho(\boldsymbol{r}_{BCP})$: charge density at the BCP in e Å^{-3}; $\nabla^2\rho(\boldsymbol{r}_{BCP})$: Laplacian of $\rho(\boldsymbol{r})$ at the BCP in e Å^{-5}; ε_{BCP}: ellipticity of $\rho(\boldsymbol{r})$ at the BCP.

The values of the S–C single bond are in the expected range with a bond length of 1.8161(2) Å, $\rho(\boldsymbol{r}_{BCP}) = 1.45(2)$ e Å^{-3}, $\nabla^2\rho(\boldsymbol{r}_{BCP}) = -8.01(4)$ e Å^{-5}, and $\varepsilon_{BCP} = 0.09$.[15] The two formal S1=N2,3 bond lengths of 1.5278(2) and 1.5179(2) Å, respectively, are in the range normally quoted for S=N bonds.[16] The S1–N1 bond in **2** of 1.6494(2) Å is comparable to that in S_4N_4 (1.629(1) Å), which was interpreted as a shortened S–N single bond with π contribution ($\varepsilon_{BCP} = 0.17$).[17] Bader et al. found in their pioneering theoretical study, electron-density features (two bonded and two nonbonded *v*alence *s*hell *c*harge *c*oncentrations (VSCCs), at nitrogen), which persuaded them to formulate the S–N bond in S_4N_4 as a S^+–N^- bond.[18] The marginal elongation of the S1–N1 bond in **2** can be attributed to the participation of N1 in the hydrogen bonding. Nevertheless, this bond displays the expected features of a covalent S–N single bond ($\rho(\boldsymbol{r}_{BCP}) = 1.89(2)$ e Å^{-3}, $\nabla^2\rho(\boldsymbol{r}_{BCP}) = -13.41(7)$ e Å^{-5}) and might serve as an internal standard. The charge density and the absolute value of the negative Laplacian at the BCP of the two formal double bonds S1–N2 and S1–N3 are significantly higher than for the S1–N1 bond.

The slightly lower value of $\rho(\boldsymbol{r}_{BCP})$ for S1=N2 than for the S1=N3 bond, with the first involved in the intramolecular hydrogen bonding, demonstrates the sensitivity of the method. The differences can be assigned to charge delocalization from the S1=N2 bonding region to the N2 valence-density region that points as a charge donor to the bridging hydrogen atom. All the S–N bonds show ellipticities unequal to zero ($\varepsilon_{BCP} = 0.11$ (N1), 0.10 (N2), 0.06 (N3)). At first glance this is especially confusing for the S1–N1 bond, as high bond ellipticity is commonly assigned to π contribution in nonpolar double bonds but this bond has to be regarded unequivocally a single bond. Compared to ε_{BCP} of N1 the values of the ellipticity for the formal double bonds are remarkably low. An investigation of the distribution of the negative Laplacian, $-\nabla^2\rho(\boldsymbol{r})$, uncovers an alternative explanation than the π contribution for the nonvanishing ellipticities.

Beside a critical-point search in $\rho(\boldsymbol{r})$, which leads to a characterization of bonds, we performed intensive searches for $(3,-3)$ critical points (which bear information about hybridization states) in the spatial distribution of $-\nabla^2\rho(\boldsymbol{r})$ to locate and quantify nonbonding VSCCs around the nitrogen atoms. Isosurfaces around the nitrogen atoms and contour plots which show the distribution of $-\nabla^2\rho(\boldsymbol{r})$ in planes containing the $(3,-3)$ critical points are presented in Figure 2.

The analysis of the Laplacian distribution around the nitrogen atoms indicates that they are sp^3 hybridized. As expected N1 shows one and both other, formally double-bonded nitrogen atoms, show two separated $(3,-3)$ critical points in $-\nabla^2\rho(\boldsymbol{r})$. The lone pair VSCC at N1 indicates concentration at the apical position of a trigonal-pyramidal coordinated sp^3-hybridized nitrogen atom (Figure 2, left), but it is oriented towards the bonding region of the S–N bond, as demonstrated by the small angle of 87.0° to the S1–N1 bond. This feature explains the considerable ellipticity of the S1–N1 bond. The VSCCs at N3 in the lone-pair regions affirm the

  1433-7851/02/4112-2080 $ 20.00+.50/0 *Angew. Chem. Int. Ed.* **2002**, *41*, No. 12

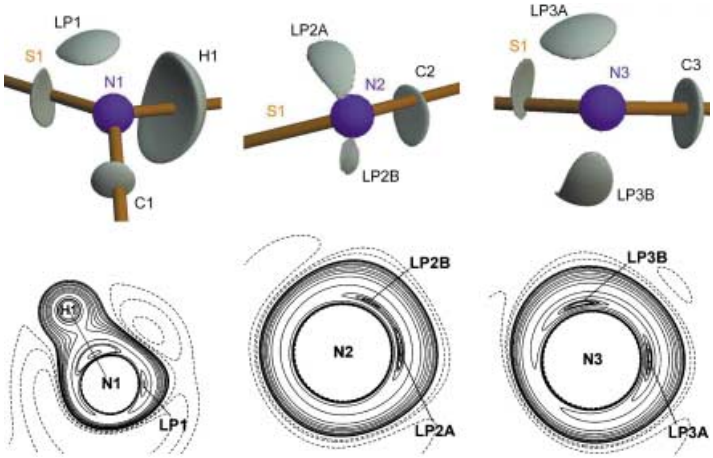

Figure 2. Isosurface map at constant $-\nabla^2\rho(\boldsymbol{r})$ values indicating bonded and nonbonded charge concentrations around N1, N2, and N3 ($-\nabla^2\rho(\boldsymbol{r}) = 47$ e Å^{-5} for N1, 48 e Å^{-5} for N2, and 46 e Å^{-5} for N3) and contour plots of charge concentrations in the H1-N1-LP1, LP2A-N2-LP2B, and LP3A-N3-LP3B plane. Maxima of the nonbonding VSCCs (lone pairs) are labeled LP. Positive values of $\nabla^2\rho(\boldsymbol{r})$ are marked by dashed lines, negative values by solid lines. Angles with lone-pair participation [°]: LP1-N1-H1 119.2, LP2A-N2-LP2B 62.8, LP3A-N3-LP3B 102.2. The angles between the normal vectors of the LP1-N1-H1 plane as well as between the LP2,3A-N2,3-LP2,3B planes and the accompanying S–N and C–N bonding vectors are 105.4° and 129.7° at N1, 99.1° and 137.9° at N2, and 107.1° and 126.8° at N3. This situation clearly indicates the orientation of the lone pairs away from the C–N towards the S–N bonding regions.

sp^3 character of N3 as the maxima in $-\nabla^2\rho(\boldsymbol{r})$ and are located above and below the S-N-C plane (Figure 2, right) with an LP3A-N3-LP3B angle of 102.2°. This angle along with the S1-N3-C3 bond angle of 126.6(1)° causes a rather distorted tetrahedral environment at N3. However, the angle between N3 and the two related BCPs is only 122.0°. This smaller angle confirms the steric strain between the *tert*-butyl group and the sulfur atom which leads to the increase of the angle from that expected for ideal tetrahedral geometry. Two maxima in $-\nabla^2\rho(\boldsymbol{r})$ are resolved in the nonbonding region at N2. The situation is similar to N3 (S1-N2-C2 123.4(1)° and BCP-N2-BCP 118.1°), although because of hydrogen bonding the maxima are less-well separated. The LP2A-N2-LP2B angle is only 62.8° because both lone-pair VSCCs at N2 interact like a bifurcated hydrogen bond (LP2A $\cdots$ H4 1.75 and LP2B $\cdots$ H4 1.91 Å) to the opposite H4 contracting the angle considerably. It is clear that all nonbonding VSCCs bend towards the associated S–N bond, as shown by the angle differences between the S–N and C–N bonds and the normal vectors of the LP-N-LP planes, which indicates the orientation of the lone pairs away from the C–N towards the S–N bonding regions (137.9°/99.1° at N2 and 126.8°/107.1° at N3). This situation causes additional an electron-density shift in the bond and leads to relatively high $\rho(\boldsymbol{r}_{BCP})$ values, a prominent negative Laplacian at the BCP, and substantial ellipticities.

Considering all the electronic features discussed above we conclude that the S–N/S=N bonding situation in **2** is much better described as a S$^+$–N$^-$ bond which is shortened by reinforcement resulting from orientation of the nitrogen lone pair towards the positively charged sulfur atom. This investigation confirms that neither valence expansion nor d-orbital contribution at the sulfur atom is required to explain the short S–N distances. This situation was predicted by computational methods more than fifteen years ago.[18, 19]

Experimental Section

All manipulations were performed under an inert-gas atmosphere of dry N_2 with Schlenk techniques or in an argon glovebox. All solvents were dried over Na/K alloy and distilled prior to use. ^{1}H, ^{7}Li, and ^{13}C NMR spectra were recorded in C_6D_6 (^{1}H: C_6HD_5: $\delta = 7.15$ ppm; ^{13}C C_6D_6: $\delta = 128.0$ ppm) using a Bruker AMX 400 spectrometer. IR spectra was recorded onto a Bruker IFS 25 FT-IR spectrometer. Elemental analyses were performed by the Microanalytisches Labor der Universität Würzburg.

1: A 1.6 M MeLi solution in diethyl ether (15.3 mL) was added dropwise to a solution of tri(*tert*-butyl)sulfurtriimide (6.00 g, 24.45 mmol) in THF (20 mL). The color of the solution changed instantaneously from yellow to colorless. After 3 h of stirring another of a 1.6 M MeLi solution in diethyl ether (15.3 mL) was added. Immediate evolution of methane gas was observed. After 1 h tri(*tert*-butyl)sulfurtriimide (6.00 g, 24.45 mmol) in THF (20 mL) was added dropwise. 50 % of the THF was removed in vacuum. After storage of the clear solution at -26 °C for 3 days colorless crystals were obtained (15.9 g, 88 %, m.p. 133 °C). ^{1}H NMR (400 MHz, C_6D_6): $\delta = 1.28$ (8 H, THF), 1.62 (s, 54 H, N*t*Bu), 3.52 (8 H, THF), 5.00 ppm (s, 2 H, SCH_2S); ^{13}C NMR (100 MHz, C_6D_6): $\delta = 25.35$, 68.40 (THF), 33.54 (C(CH_3)$_3$), 53.89 (C(CH$_3$)$_3$), 86.89 ppm (SCH_2S); ^{7}Li NMR (155.5 MHz, external reference saturated LiCl solution) $\delta = 1.15$ ppm; elemental analysis (%) calcd: C 60.45, H 10.97, N 11.44, S 8.72; found C 59.95, H 10.65, N 12.01, S 9.01.

2: **1** (15.9 g, 23.85 mmol) in THF was added to a suspension of *t*BuNH$_3$Cl (2.60 g, 23.85 mmol) in THF (15 mL). The solution was stirred for 3 h. THF was removed under vacuum and hexane (25 mL) was added. The precipitated LiCl was removed by filtration. 50 % of the solvent was removed under vacuum. After storage of the clear solution at -26 °C for 3 days colorless crystals were obtained (8.3 g, 69 %, m.p. 128 °C). ^{1}H NMR: (400 MHz, C_6D_6) $\delta = 1.41$ (s, 18 H, NHCCH_3), 1.49 (s, 36 H,=NCCH_3), 4.11 (s, 2 H, SCH_2S), 6.85 ppm (s, 2 H, N*H*CCH$_3$); ^{13}C NMR (100 MHz, C_6D_6): δ 30.95 (NHC(CH_3)$_3$), 32.31 (=NC(CH_3)$_3$), 51.82 (NHC(CH$_3$)$_3$), 53.38 (=NC(CH$_3$)$_3$), 75.90 (SCH$_2$S); IR (Nujol): 3146.7 m N(H), 3070–2860 s (Nujol), 1457.4 s, 1385.6 s, 1355.3 s, 1251.9 s, 1218.8 s, 1117.9 cm^{-1} s; elemental analysis (%) calcd: C 59.23, H 11.53, N 16.58, S 12.65; found C 59.95, H 11.65, N 16.01, S 13.01.

Received: October 15, 2001
Revised: March 15, 2002 [Z18068]

[1] a) K. Magnus, *Liebigs Ann. Chem.* **1833**, *6*, 152; b) J. von Liebig, *Liebigs Ann. Chem*. **1835**, *13*, 35; c) A. Strecker, *Liebigs Ann. Chem.* **1868**, *148*, 90; d) H. J. Backer, *Recl. Trav. Chim. Pays-Bas Belg.* **1929**, *48*, 949.
[2] T. L. Smith, J. H. Elliott, *J. Am. Chem. Soc.* **1953**, *75*, 3566.
[3] a) D. Mootz, H. Wunderlich, *Acta Crystallogr. Sect. B*, **1970**, *26*, 1820; b) P. Sartori, R. Jüschke, R. Boese, D. Bläser, *Z. Naturforsch. B*, **1994**, *49*, 1467.
[4] For example, a) F. Charbonnier, R. Faure, H. Loiseleur, *Acta Crystallogr. Sect. B*, **1979**, *35*, 1773; b) A. Karipides, *Acta Crystallogr. Sect. B*, **1981**, *37*, 2232; c) M. R. Truter, *J. Chem. Soc.* **1962**, 3393.
[5] V. A. Russell, C. C. Evans, W. Li, M. D. Ward, *Science* **1997**, *276*, 575.
[6] Review: a) R. Fleischer, D. Stalke, *Coord. Chem. Rev.* **1998**, *176*, 431; S(NR)$_3^{2-}$: b) R. Fleischer, S. Freitag, F. Pauer, D. Stalke, *Angew. Chem.* **1996**, *108*, 208; *Angew. Chem. Int. Ed. Engl.* **1996**, *35*, 204; S(NR)$_4^{2-}$: c) R. Fleischer, A. Rothenberger, D. Stalke, *Angew. Chem.* **1997**, *109*, 1140; *Angew. Chem. Int. Ed. Engl.* **1997**, *36*, 1105.
[7] T. S. Koritsanszky, P. Coppens, *Chem. Rev.* **2001**, *101*, 1583.
[8] B. Walfort, D. Stalke, *Angew. Chem.* **2001**, *113*, 3965; *Angew. Chem. Int. Ed.* **2001**, *40*, 3846.
[9] B. Walfort, A. P. Leedham, C. A. Russell, D. Stalke, *Inorg. Chem.* **2001**, *40*, 5668.

  1433-7851/02/4112-2081 $ 20.00+.50/0

[10] Crystal data for **1** and **2** (conventional/IAM refinement): The data were collected from shock-cooled crystals for **1** on an ENRAF-NONIUS CAD4 diffractometer and for **2** on an BRUKER APEX diffractometer (graphite-monochromated $Mo_{K\alpha}$ radiation, $\lambda = 0.71073$ Å) equipped with a low-temperature device at 193(2) K (**1**) and 100(2) K (**2**).[20] The structures were solved by direct methods (SHELXS-97)[20] and refined by full-matrix least-squares methods against F^2 (SHELXL-97).[22] R values defined as $R1 = \Sigma||F_o| - |F_c||/\Sigma|F_o|$, $wR2 = [\Sigma w(F_o^2 - F_c^2)^2/\Sigma w(F_o^2)^2]^{0.5}$, $w = [\sigma^2(F_o^2) + (g_1P)^2 + g_2P]^{-1}$, $P = 1/3[\max(F_o^2,0) + 2F_c^2]$. **1**: $C_{37}H_{80}Li_2N_6O_3S_2$, $M_r = 735.07$, monoclinic, space group $P2_1/c$, $a = 16.143(8)$, $b = 14.5340(18)$, $c = 19.429(8)$ Å, $\beta = 92.779(18)$, $V = 4553(3)$ Å^3, $Z = 4$, $\rho_{calcd} = 1.072$ Mg m^{-3}, $\mu = 0.155$ mm^{-1}, $F(000) = 1624$, 10144 reflections measured, 5527 unique, $R(\text{int}) = 0.0660$, $wR2$ (all data) $= 0.1768$, $R1(I > 2\sigma(I)) = 0.0639$, $g_1 = 0.0695$, $g_2 = 9.0558$ for 602 parameters and 566 restraints. **2**: $C_{25}H_{58}N_6S_2$, $M_r = 506.89$, monoclinic, space group $C2/c$, $a = 29.8239(8)$, $b = 11.4206(3)$, $c = 18.0801(4)$ Å, $\beta = 91.041(1)$, $V = 6157.2(3)$ Å^3, $Z = 8$, $\rho_{calcd} = 1.094$ Mg m^{-3}, $\mu = 0.196$ mm^{-1}, $F(000) = 2256$, 136761 reflections measured (low-angle batch, $\sin\theta/\lambda < 0.625$ Å^{-1}), 6629 unique, $R(\text{int}) = 0.0435$, 217620 reflections measured (high-angle batch, 0.625 Å$^{-1} < \sin\theta/\lambda < 1.111$ Å^{-1}), 29791 unique, $R(\text{int}) = 0.0646$, $wR2$(all data) $= 0.0932$, $R1(I > 2\sigma(I)) = 0.0315$, $g_1 = 0.0538$, $g_2 = 0.0$ for 475 parameters. All hydrogen atoms in **2** were located by difference Fourier synthesis and refined without any distance restraints. The isotropic thermal parameters of the hydrogen atoms H1 and H4 were refined independently. All other hydrogen atoms of the molecule were refined using a riding model ($U_{iso} = 1.2\,U_{eq}$ (C) for H71 and H72 and $U_{iso} = 1.5\,U_{eq}$ (C) for all other hydrogen atoms). CCDC-171900 (**1**) and CCDC-171901 (**2**) contain the supplementary crystallographic data for this paper. These data can be obtained free of charge via www.ccdc.cam.ac.uk/conts/retrieving.html (or from the Cambridge Crystallographic Data Centre, 12, Union Road, Cambridge CB2 1EZ, UK; fax: (+44) 1223-336-033; or deposit @ccdc.cam.ac.uk).

[11] N. K. Hansen, P. Coppens, *Acta Crystallogr. Sect. A* **1978**, *34*, 909.

[12] T. Koritsanszky, S. Howard, T. Richter, Z. W. Su, P. R. Mallinson, N. K. Hansen, *XD—A Computer Program Package for Multipole Refinement and Analysis of Electron Densities from Diffraction Data*, Freie Universität Berlin, **1995**

[13] Multipole refinement of **2**: data integration was performed with SAINT-NT,[23] empirical absorption correction based on Blessing's algorithm[24] with MULABS implemented in PLATON:[25] $R(\text{int}) = 0.0435$ (low-angle batch), $R(\text{int}) = 0.0646$ (high-angle batch), structure solution with SHELXS,[21] high-order refinement with SHELXL-97;[22] $wR1 = 0.0147$, $wR2 = 0.0280$, GoF $= 1.3015$, after multipole refinement. In the refinement both $S(NHtBu)(NtBu)_2$ moieties at the methylene bridge shared the same multipole parameters. In the pseudoatom model the deformation density was described by an expansion over spherical harmonics multiplied by Slater-type radial functions with energy-optimized exponents.[26] Atomic densities were expanded to hexadecapolar level for S, N, and C7, octapolar level for all other carbon atoms, for H atoms one bond-directed dipole as well as a quadrupole population were employed. The final difference Fourier syntheses after multipole refinement are virtually featureless.

[14] R. F. W. Bader, *Atoms in Molecules—A Quantum Theory*, Clarendon Press, Oxford **1990**.

[15] S. Pillet, M. Souhassou, Y. Pontillon, A. Caneschi, D. Gatteschi, C. Lecomte, *New J. Chem.* **2001**, *25*, 131.

[16] P. Rademacher, *Strukturen organischer Moleküle*, VCH, Weinheim **1987**.

[17] W. Scherer, M. Spiegler, B. Pedersen, M. Tafipolsky, W. Hieringer, B. Reinhard, A. J. Downs, G. S. McGrady, *Chem. Commun.* **2000**, 635.

[18] T.-H. Tang, R. F. W. Bader, P. J. MacDougall, *Inorg. Chem.* **1985**, *24*, 2047.

[19] a) W. Kutzelnigg, *Angew. Chem.* **1984**, *96*, 262; *Angew. Chem. Int. Ed. Engl.* **1984**, *23*, 272; b) A. E. Reed, F. Weinhold, *J. Am. Chem. Soc.* **1986**, *108*, 3586; c) D. A. Bors, A. Streitwieser, *J. Am. Chem. Soc.* **1986**, *108*, 1397; d) A. E. Reed, P. v. R. Schleyer, *J. Am. Chem. Soc.* **1990**, *112*, 1434; e) U. Salzner, P. v. R. Schleyer, *J. Am. Chem. Soc.* **1993**, *115*, 10231; f) T. Stefan, R. Janoschek, *J. Mol. Model.* **2000**, *6*, 282.

[20] D. Stalke, *Chem. Soc. Rev.* **1998**, *27*, 171.

[21] G. M. Sheldrick, *Acta Crystallogr. Sect. A* **1990**, *46*, 467.

[22] G. M. Sheldrick, SHELXL-97—Program for Crystal Structure Refinement, University of Göttingen, **1997**.

[23] Bruker Nonius Inc., *SAINT-NT*—Program for Integration of Diffraction Data from Area Detectors, Madison WI **2000**.

[24] B. Blessing, *Acta Crystallogr. Sect. A* **1995**, *51*, 33.

[25] A. L. Spek, *Acta Crystallogr. Sect. A* **1990**, *46*, C34.

[26] E. Clementi, C. Roetti, *At. Data Nucl. Data Tables*, **1974**, *14*, 177

Structural Dependence of Redox-Induced Dimerization as Studied by In Situ ESR/UV/Vis-NIR Spectroelectrochemistry: The Fluoranthenopyracylene Oligomers**

Lothar Dunsch,* Peter Rapta, Niels Schulte, and A. Dieter Schlüter

Reversible dimerization reactions of electrochemically produced organic radical ions are used as a general model for the explanation of charge injection in conducting oligomers and polymers.[1–4] Our main interest in this field is to investigate the driving force of dimerization in such structures. While detailed electrochemical and spectroscopic studies of conjugated compounds have been presented by several groups,[5–11] the number of in situ spectroelectrochemical investigations resulting in more direct information on the structural situation during dimerization is limited and the formation of σ dimers has not been demonstrated by in situ techniques. Furthermore, a variety of structures is needed to understand the dimerization as a general reaction of oligomeric systems. Thus monodisperse organic compounds with low molecular weight such as naphthalene diimides,[5] thianthrenes,[6] bipyrrols,[7] bithiophenes,[8] and extended conjugated oligomers, for example, oligothiophenes,[9] oligophenylenes,[10] and oligopyrroles[11] were used for such studies.

For structural studies of the reaction products at electrode surfaces the spectroelectrochemical techniques (including ESR/UV/Vis-NIR spectroscopy at different temperatures) were applied.[12] The existence of both π and σ dimers of oligopyrrols after a charge-transfer reaction has been dem-

[*] Priv.-Doz. Dr. L. Dunsch, Dr. P. Rapta[+]
IFW Dresden
Abteilung Elektrochemie und leitfähige Polymere
Helmholtzstrasse 20, 01069 Dresden (Germany)
Fax: (+49) 351-4659-745
E-mail: l.dunsch@ifw-dresden.de
Dr. N. Schulte, Prof. Dr. A. D. Schlüter
Institut für Chemie, Freie Universität Berlin
Takustrasse 3, 14195 Berlin (Germany)

[+] Permanent address:
Slovak University of Technology
Radlinského 9, 812 37 Bratislava (Slovakia)

[**] This work was supported by the Deutsche Forschungsgemainschaft. PR thanks Humboldt Foundation and Slovak Grant Agency for financial support. The authors thank Dr. M. Breza (STU Bratislava) for quantum-chemical calculations.

  1433-7851/02/4112-2082 $ 20.00+.50/0